# HapCube: A Wearable Tactile Device to Provide Tangential and Normal Pseudo-Force Feedback on a Fingertip

**Hwan Kim, HyeonBeom Yi, Hyein Lee, and Woohun Lee**
Department of Industrial Design, KAIST
291 Daehak-ro, Yuseong-gu, Daejeon, South Korea
{hwan.kim, hyeonbeom, hyein.l, woohun.lee}@kaist.ac.kr

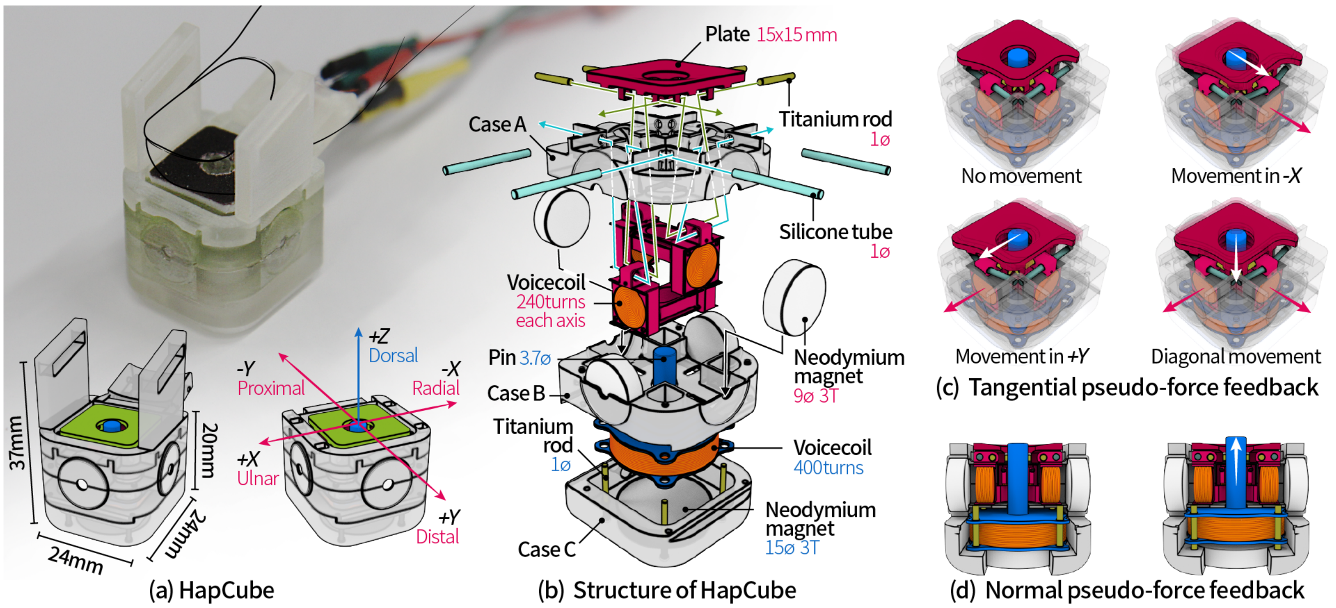


**Figure 1. HapCube. Image of HapCube illustrating its size (a) and it structure (b). Apart from the accessory components for wearing, the weight is 19g. The plate moves in any tangential directions (c), and the pin moves in the normal direction (d).**


## ABSTRACT
Haptic devices allow a more immersive experience with Virtual and Augmented Reality. However, for a wider range of usage they need to be miniaturized while maintaining the quality of haptic feedback. In this study, we used two kinds of human sensory illusion of vibration. The first illusion involves creating a virtual force (pulling sensation) using asymmetric vibration, and the second involves imparting compliances of complex stress-strain curves (i.e. force-displacement curves of mechanical keyboards) to a rigid object by changing the frequency and amplitude of vibration. Using these two illusions, we developed a wearable tactile device named HapCube, consisting of three orthogonal voicecoil actuators. Four measurement tests and four user tests confirmed that 1) a combination of two orthogonal asymmetric vibrations could provide a 2D virtual force in any tangential directions on a finger pad, and 2) a single voicecoil actuator produced pseudo-force feedback of the complex compliance curves in the normal direction.



ACM 978-1-4503-5620-6/18/04…$15.00
https://doi.org/10.1145/3173574.3174075


### Author Keywords
Haptics; haptic illusion; asymmetric vibration; compliance; wearable devices.

### ACM Classification Keywords
H.5.2. Information interfaces and presentation: User Interfaces – Haptic I/O


## INTRODUCTION
As the virtual and augmented reality (VR and AR) markets mature, users are seeking more realistic experiences than simply visual ones, and expect to touch and feel virtual images by their own hands, as in science fiction movies. In recent years, to keep pace with the markets and user expectations, research on the miniaturization of wearable haptic devices for end users has become necessary and is being conducted steadily.

The use of vibration is one of the most promising approaches for miniaturization, because of the small size of vibration motors (e.g., voicecoil actuator). Many wearable haptic devices using vibration have been proposed, and most of them are much smaller and lighter than the other types of haptic devices such as grounded haptic devices [25,38], and exoskeleton gloves [7]. However, most of their vibrotactile feedback still provide only binary information about the transition between the touched and released states [15,18]; they do not satisfy user expectations at all. Vibration has a great advantage for miniaturization, but it needs a way to sufficiently utilize the sensitive and sophisticated human tactile system.

Recently, two remarkable new discoveries of 'vibration and human sensory illusion' were made, based on which methods have been proposed to create pseudo-force sensation using vibration. The first discovery is that asymmetric vibration results in pulling sensation in a certain direction [1,2,27], which feels like frictional force. The second is that changes in the frequency and amplitude of vibration impart compliances of complex stress–strain curves (e.g., force–displacement curves of Cherry keyboards [8]) to a rigid object[21,23]. These discoveries allow the use of vibration to provide pseudo-force feedback, rather than simply informing about the state transition. In addition, these two findings are worth exploring further, because vibration motors can be conveniently miniaturized to a size that permits the design of a wearable device.

We designed a wearable tactile device named HapCube based on these two discoveries in order to investigate the possibilities of the discoveries. It provides tangential pseudo-force feedback (two degrees of freedom (DoFs) in the *XY* plane) and normal pseudo-force feedback (one-DoF in the *z*-axis) to the user's finger pad. The two orthogonal voicecoil actuators shown in Figure 1(c) oscillate the plate asymmetrically, and it renders virtual forces in any direction on the *XY* plane. The voicecoil actuator shown in Figure 1 (d) moves up and down to provide normal pseudo-force feedback to the finger pad.

In this study, we first attempted to determine if it was feasible to combine the two orthogonal asymmetric vibrations to produce a 2D virtual force, and if humans could perceive its direction correctly. Secondly, it was investigated whether the normal pseudo-force feedback of HapCube could simulate various compliance curves and be distinguishable. The possibility of interference between the two feedbacks when the feedbacks are generated simultaneously was also investigated. To achieve these, we performed four measurement tests and four user tests.

## RELATED WORK

### Asymmetric Vibration and Virtual Force

Asymmetric vibration is an oscillation involving fast movement in the positive direction and slow movement in the negative direction, which stimulates the human mechanoreceptors and makes a pulling sensation (pseudo-force) along the positive direction. In 2005, Amemiya et al. designed a hand-held haptic device with a slider-crank mechanism to generate asymmetric vibration and observed this phenomenon; they named the pulling sensation as "virtual force" [1].

After Rekimoto [27] and Amemiya & Gomi [2] proposed a method to create a virtual force using commercial voicecoil actuators, various studies on the asymmetric vibration in Haptics and Human–Computer Interactions were conducted. A method using a small-sized speaker rather the voicecoil actuator has been proposed [35], and Tanabe et al. [36] demonstrated the feasibility of providing a one-DoF translational cue and a one-DoF rotational cue with two speakers arranged in a staggered manner. Moreover, since a method to create virtual torque by asymmetrically moving a flywheel was proposed [3,10], asymmetric vibration could be equally applied to rotational movement as well as transitional movement. Recently, there have been attempts to clarify the principle of virtual force by analyzing the mechanical relationship between asymmetric vibration and finger skin. They suggest that asymmetric skin displacement stimulates mechanoreceptors asymmetrically, and stimuli in the positive direction mask stimuli in the negative direction, which results in continuous pulling sensation [12,19].

There have been attempts to apply various asymmetric vibrations; however, a suitable solution for expanding one-dimensional virtual forces into multi-dimensional virtual forces by synthesizing orthogonal vibrations has not been proposed. Rekimoto [27] attempted to create a 2D virtual force by simply attaching two vibrators to each other perpendicularly; however, the user test result was inferior. Culbertson et al. [13] proposed a method to provide three-DoF translation and three-DoF rotation cues by attaching several actuators to two or three fingers. However, for the users to recognize the direction and rotation cues, it is necessary to interpret all the vibrations of the actuators comprehensively. Therefore, this method is not suitable for synthesizing two orthogonal virtual forces at one point. Amemiya et al. [4] attempted to extend this to two-dimensions by rotating the slider–crank unit with a motor and demonstrated that. The just-noticeable difference in angle between the two separate virtual forces was approximately 23–30°. It is a case of successful creation of a 2D virtual force; however two perpendicular virtual forces cannot be synthesized with this method. Moreover, it is challenging to make it as small as a fingertip because it requires a motor-encoder system for changing the direction.

### Vibration and Compliance

The capability of vibration to impart compliance to a rigid surface was first reported in a study by Kildal in 2010 [21]. He categorized human haptic sensation perceived while pressing compliant material into kinesthetic sensation (when pressing a spring) and cutaneous sensation (vibration caused by friction). He verified that an individual perceived a rigid object to be elastic when an additional vibrotactile cue simulating the vibration was provided. Strohmeier et al. [33] proposed a bendable smartphone prototype that utilized

Kildal's method to support user's bending input. Kim and Lee [23] proposed a method to simulate various compliances of physical switches based on their own force–displacement curves. When an individual presses a rigid object, changes in the frequency and amplitude of vibration create virtual haptic switch sensations.

Kim et al. [22] designed a wearable haptic device using the method of Kildal and Kim and Lee. The device consists of a servo motor for providing kinesthetic feedback to the finger and a linear resonant actuator for generating vibration. This study empirically demonstrated that the device could provide feedback with higher accuracy by supplementing the kinesthetic feedback with vibrotactile feedback. It is necessary to confirm that their method works when stimulating only the cutaneous sensation (excepting kinesthesia). Moreover, it is challenging to use the device as a wearable haptic device because of the configuration using servo motor and the shape covering the whole finger.

### Multi-DoF Pseudo-Force Actuators

HapCube is a kind of voicecoil actuator like Haptuator [39]; however HapCube has three voicecoil actuators placed in a small space and is designed as a moving-coil actuator to minimize magnetic interference between the actuators (because electromagnets are usually much weaker than neodymium magnets). Since the coil is lighter than the magnet, under the same conditions, the vibration power of the moving-coil actuator is weaker than that of a moving-magnet actuator such as the Haptuator. Therefore, we designed a structure that does not vibrate the entire HapCube device but only the plate.

Finger-worn tactile devices that provide 3-DoF pseudo-force feedback using a moving platform have been proposed [9,26,31,32]. The most recent work among them is the 3-DoF tactile device proposed by Schorr & Okamura [31]. Its moving space is 10 × 10 × 5 mm, and it can apply a force of up to 7.5 N by using small DC motors and mechanical linkages. They deform the skin of the finger pad in a manner similar to object manipulation; therefore they seem to use the high resolution of the slowly adaptive receptors (i.e., Merkel's disk, and Ruffini's ending) very well.

However, there are only few studies on moving platform devices that provide haptic feedback by stimulating the rapidly adaptive receptors (i.e., Meissner's, and Pacinian corpuscles). It requires only a rapid change of force and displacement, not a large force and displacement to stimulate these receptors. The working space of HapCube is only 2 × 2 × 1 mm, and the maximum force is only 0.4 N; however, it was designed to utilize vibration and the two rapidly adaptive receptors.

In this study, we propose a prototype called HapCube. With this prototype, we verify whether 1) a 2D virtual force feedback can be generated by synthesizing two orthogonal virtual forces, and 2) whether pseudo-force feedback can simulate the complex compliance curves with a single voicecoil actuator.

## HAPCUBE DESIGN

HapCube is a wearable tactile device in the form of a cube. It provides 2D virtual force feedback obtained by merging two asymmetric vibrations in the tangential direction of the finger pad, and 1-DoF pseudo-force feedback with various compliance patterns using a small-sized voicecoil actuator in the normal direction (Figure 1). It is made using a 3D printer (Projet 3500 HDMax), and its dimensions are 24 × 24 × 20 mm, excluding the accessory components for wearing, and the weight excluding the wire is 19 g.

To generate feedback in the tangential and normal directions, three electromagnets and five neodymium magnets are used. To make the magnetic field symmetric and minimize the interference between the axes, all the five magnets are aligned with the same pole facing inward. To withstand the repulsion between the magnets, the magnets and the cases are fastened with an instant adhesive.

In the tangential plane, the two electromagnets are aligned orthogonally to each other, and the move independently in the $+X$ or $-X$ and $+Y$ or $-Y$ directions, respectively, depending on whether a positive or negative voltage is applied. These two electromagnets are connected to the plate by titanium rods (titanium is paramagnetic and does not react to the magnets) and to Case A by silicone tubes, which functioning as a damper (see Figure 1 (b) and (c)). Similar to the movement of an $X$–$Y$ translation stage, the plate can move freely in any direction on the tangential plane, matching the movements of the two electromagnets (Figure 1 (c)). A piece of sandpaper is placed on the plate to increase its friction with the finger pad.

The pin attached to the bottom electromagnet can be moved in the dorsal direction ($+Z$ direction) of the finger (Figure 1 (d)). Four titanium rods are placed around the pin and electromagnet as a guide to limit the lateral movement of the pin.

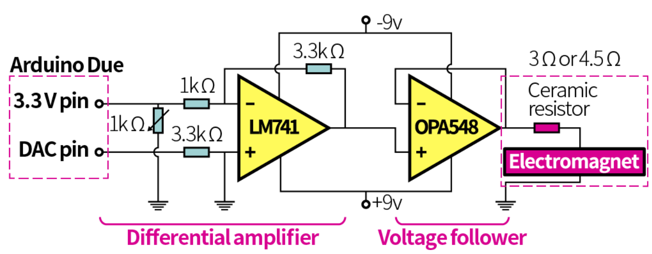


**Figure 2. Signal generation schematic**

An Arduino Due and two operational-amplifier (Op-amp; LM741, and OPA548) circuits drive each actuator (Figure 2). To move the actuator in both the positive and negative directions, the positive voltage signal (0~3.3 V) from an Arduino Due 12-bit DAC (Digital to Analog Converter) pin is amplified to a dual polarity voltage signal (± 4.9 V) through the differential amplifier circuit. Then, to drive the actuators, the current is amplified with a high-current op-amp (OPA548; maximum continuous output current: 3 A; maximum peak output current: 5 A). With the internal resistances of the actuators in the tangential plane and normal direction, the resistances of the ceramic resistors were set to 3 and 4.5 Ω, respectively.

### Tangential Feedback Design

The asymmetric vibration of the two voicecoil actuators generates the tangential feedback of HapCube. Researchers who have studied asymmetric vibration have used various drive signals to match the characteristics of the actuators used (e.g., a square wave and voicecoil actuator [2,27], a sawtooth wave and DC motor [29], and an asymmetrically modified sine wave and a speaker [35,36]). Although the drive signal required to generate a virtual force must be determined experimentally, two guidelines for higher virtual force are known from previous studies. One is that it is more effective to use a signal with a frequency that stimulates the Meissner corpuscle rather than the Pacinian corpuscle (between 10 and 50 Hz) [2], and the other is to reduce the restoring force to slow the movement in the negative direction [12].

The signal for the feedback was designed through an empirical process as shown on the left in Figure 3, which consists of (a) positive acceleration, (b) negative deceleration, and (c) pause sections. In the positive acceleration section, a current of 1.5 A (4.5 V) flows for 6 ms; this rapidly shifts the electromagnet in the positive direction. In the negative deceleration section, a current of 0.18 A (0.54 V; 12% of the voltage in the positive acceleration section) flows for 7 ms; this suppresses the restoring force of the silicone tubes. Then, no current flows for 7 ms in the pause section. This signal produces an asymmetric vibration of 50 Hz; the changes in the acceleration and position of the voicecoil actuator are shown on the center and right in Figure 3 (Refer to the Tangential Vibration Measurement section for the measurement process). The maximum values of acceleration and position in the positive direction were 2.5 g (24.5 $\mathrm{m}/s^2$) and 0.29 mm, respectively, and the maximum values in the negative direction were -1.8 g (17.7 $\mathrm{m}/s^2$) and - 0.18 mm.

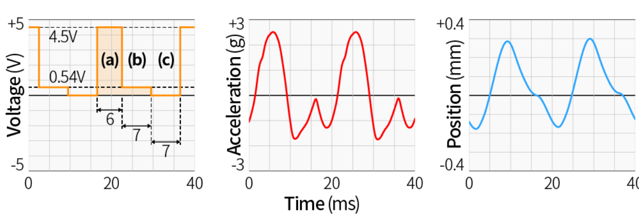


**Figure 3. Tangential feedback signal design. The driving signal (left), acceleration changes (center), and position changes (right) of the voicecoil actuator on the *x*-axis.**

When an identical signal is provided, the *y*-axis vibration is marginally weaker than the *x*-axis vibration. To rectify this, we provided a maximum signal (4.275 V ($V_{xMax}$)) to the *x*-axis electromagnet and a maximum signal (4.5 V ($V_{yMax}$)) to the *y*-axis electromagnet.

The two actuators move independently in each orthogonal direction permitting the plate to move in any direction on the tangential plane. To move the plate at any angle ($\theta$) from the +*x*-axis, the voltages ($V_x$ and $V_y$) of the positive acceleration section are determined by the following formula:

$$V_x = V_{xMax} \times \cos\theta, \quad V_y = V_{yMax} \times \sin\theta \qquad (1)$$

The voltage of the negative deceleration section is 12% of the voltage of the positive acceleration section.

### Normal Feedback Design

Before designing the normal feedback, it is necessary to determine the relationship between the force and voltage. Figure 4 (a) shows the linear relationship between them. When the voltage was divided into 1000 steps from 0 to 4.5 V and gradually increased, the force applied by the pin was measured by a load cell (Refer to the Normal Force Measurement section for the detailed measurement process). From five repeated measurements, it is observed that force and voltage exhibit a linear relationship (linear regression test; $Force\ (cN) = -0.668 + 9.377 \times Voltage\ (V)$, $R^2 = .976, p < .05$). When the maximum voltage (4.5 V) was applied, the maximum force was approximately 41.5 cN.

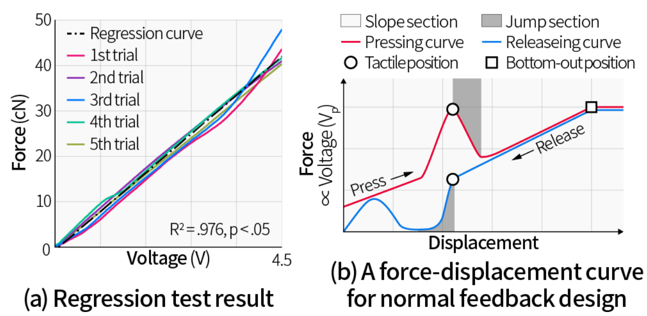


**Figure 4. Regression test result (a) and a force–displacement curve for normal feedback design (b).**

The normal feedback is determined by using a force–displacement curve, assuming that force–voltage is in a linear relationship. Figure 4 (b) shows the force–displacement curve of CHERRY Blue key switch [8]. When we press the key switch, the repulsive force of the key changes according to the displacement of the key and the pressing curve (red line). When the finger passes between the peak point (tactile position) of the pressing curve and the end of the downhill slope, users will perceive an abrupt collapse of the key. We divide this section into a jump section (gray area) and a slope section (white area). After the key reaches the bottom-out position, the repulsive force changes according to the releasing curve (blue line). The releasing curve is also divided into a jump section, where the force weakens abruptly, and a slope section.

The division of these sections is marginally different from that of Kim and Lee [23]. They set the jump section from the tactile position to the subsequent position at which it is restored to its height. This required determination of the point at which the vibration pattern was to be changed according to the pressing force measured by a pressure sensor, rather than the displacement. Therefore, they set the end of the jump section to a position as high as the tactile position's height; the width of their jump section was larger than that of our jump section. Kim et al. [22] applied their method to wearable haptic devices; however, they used the method without any modification. We set the jump section to include only the section where the user can perceive the abrupt collapse.

The voltage in the normal direction is determined by these force–displacement curves, which are designed to produce a force (that pushes the finger pad) and vibration (that creates a haptic illusion). The voltage for the pushing force ($V_p$) is determined by the force curves regardless of the section division, and the voltage for the vibration ($V_v$) is determined differently depending on the section. In a slope section, a grain vibration is generated each time a key displacement passes a grain length ($l_g$) (Figure 5 (a)). Grain vibration is a damped vibration for a period of 6 ms (166.7 Hz) that endures for three cycles; this permits the user to perceive linear elasticity. The initial amplitude of $V_v$ for this was experimentally set to 0.3 V. In the jump section, the vibration of 333.3 Hz continues until it passes from the tactile position to the end downhill. The amplitude of this jump vibration decreases as its distance from the tactile position increases (Figure 5 (b)); this provides the user the sensation of an abrupt sliding down of the fingertip. The amplitude of $V_v$ was 0.6 V at the tactile position and 0 V at the end of the jump section. When the displacement reaches the bottom-out position, a bottom-out vibration is created to generate the impression that it has hit the wall (Figure 5 (c)). The oscillation at 200 Hz, which becomes increasingly amplified, endures for 30 ms. The maximum amplitude of $V_v$ was 0.6 V. $V_v$ is specified as a square wave.

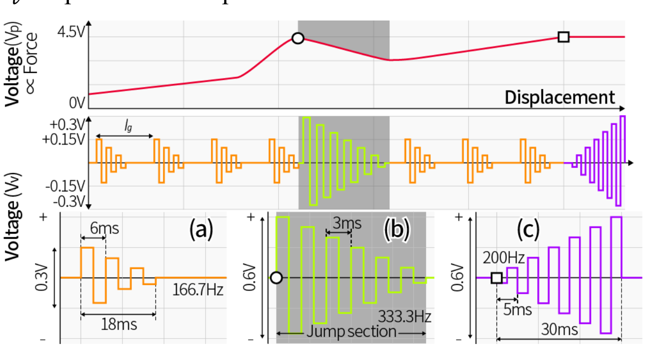


**Figure 5. Signals to generate grain vibration (a), jump vibration (b), and bottom-out vibration (c).**

The normal direction voicecoil actuator is driven by the sum of $V_p$ and $V_v$. The normal feedback of the HapCube is provided by a combination of vibration and force pressing the finger pad depending on the force–displacement curves.

## MEASUREMENT TEST

Two measurement tests were conducted to verify that the two feedbacks of the HapCube were being generated properly.

### Tangential Vibration Measurement

If the tangential feedback is generated correctly, 1) the plate should vibrate in the desired direction on the $XY$ plane, and 2) the vibration must be asymmetric. Thus, the measured vibration should satisfy the following two conditions:

1. It vibrates only in the desired direction, and there is negligible vibration in an orthogonal direction.
2. It moves rapidly in the positive direction and slowly in the negative direction.

An ADXL335 accelerometer sensor was used to measure the oscillation of the plate. For the fastest feasible data recording, the sensor value was written to a micro-SD card in binary data format using Arduino Due and Ethernet Shield 2. Binary data was recorded at 150 μs intervals, which is a sufficient writing speed to measure the tangential vibration (50 Hz).

After placing the HapCube on the fixture made for the experiment, the acceleration sensor was attached to the plate with a double-sided tape (3M double-sided form tape). The sensor and Arduino Due were connected using a thin 38 AWG enameled copper wire (diameter: approximately 0.1 mm) to minimize measurement noise due to wire weight and tension. The acceleration changes of the tangential feedback in 16 directions were measured separately, and the obtained acceleration data was used for the analysis after averaging the four proximate values. The position data was obtained by integrating the smoothed acceleration data two times over time.

#### *Results*

Figure 6 shows the change in acceleration and position of the tangential vibration in eight directions (the measurement results for all the sixteen directions can be downloaded from ACM Digital Library). The blue graph shows the position change of the plate, and the red graph shows the acceleration change. The white background graph shows the change in position and acceleration with respect to the feedback direction, and the gray background graph shows the change in position and acceleration with respect to the direction perpendicular to the feedback.

The amplitudes of the gray background graphs were negligible compare to those of the white background graphs. This implies that the vibration is generated in the desired direction (feedback direction). In the position graphs of the feedback direction, it is observed that it moves rapidly in the positive direction and slowly in the negative direction. Thus, the measurement results confirm that the tangential feedback is being generated properly.

However, vibrations in all the directions do not exhibit identical shapes. For example, the two graphs in the opposite direction (e.g., 0° and 180°) are not inverted. This is attributed to the fact that we had developed HapCube by hand (apart from the 3D printed components); it was not perfectly symmetrical. Moreover, it is observed from the diagonal (45°, 135°, 225°, and 315°) graphs that they vibrate at a higher degree in the orthogonal directions.

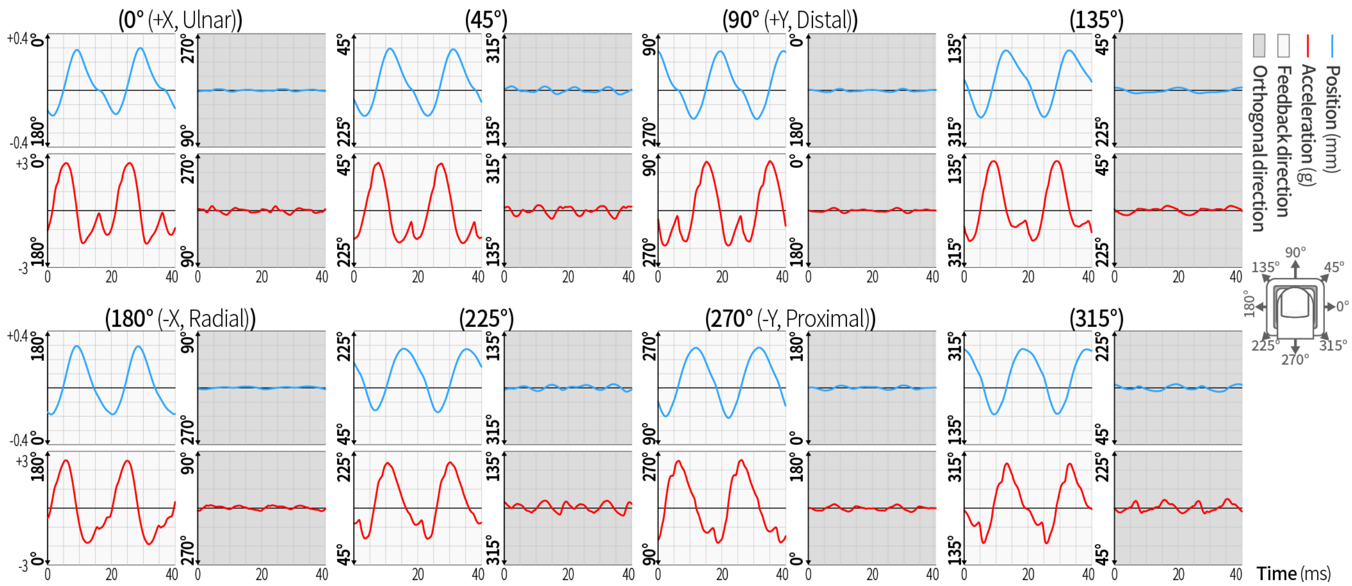


**Figure 6. Tangential vibration measurement results**

This is because the patterns of the two vibrations that produce the diagonal vibration are slightly dissimilar. For example, the amplitude of the orthogonal component of the 225° vibration is large because the two vibrations of 180° and 270°, which produce the 225° vibration, are dissimilar to each other. The accumulation of clearances that occurred during assembly appears to be another cause.

### Normal Force Measurement

It was verified whether the force component of the normal feedback along the force–displacement curves is generated effectively. The force exerted by the pin was measured using a load cell (HD-Lcell-01). The signal from the load cell was amplified by a load cell amplifier (HX711); the vibration could not be measured owing to its slow response frequency (approximately 10 Hz). Therefore, only the force from $V_p$, excluding the vibration component in the normal feedback, was measured.

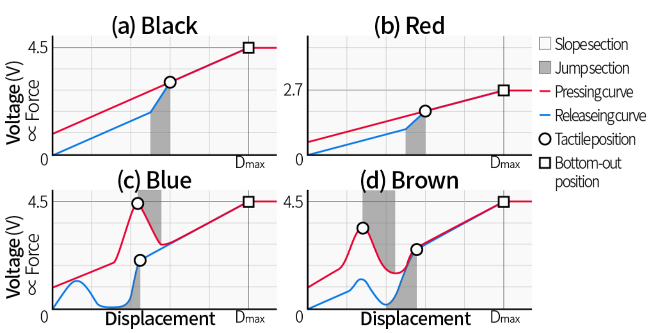


**Figure 7. Force–displacement curves for measurement test.**

The four curves shown in Figure 7 were used for the measurements, and they were derived from the force–displacement curves of the four key switches from CHERRY (**Black**, **Red**, **Blue**, and **Brown**) [8]. When the displacement was divided into 1000 steps from 0 to $D_{max}$ and gradually increased in 100 ms time intervals, the force was measured while maintaining the corresponding voltage of the curves. The pressing curve and releasing curve were measured five times separately.

*Results*

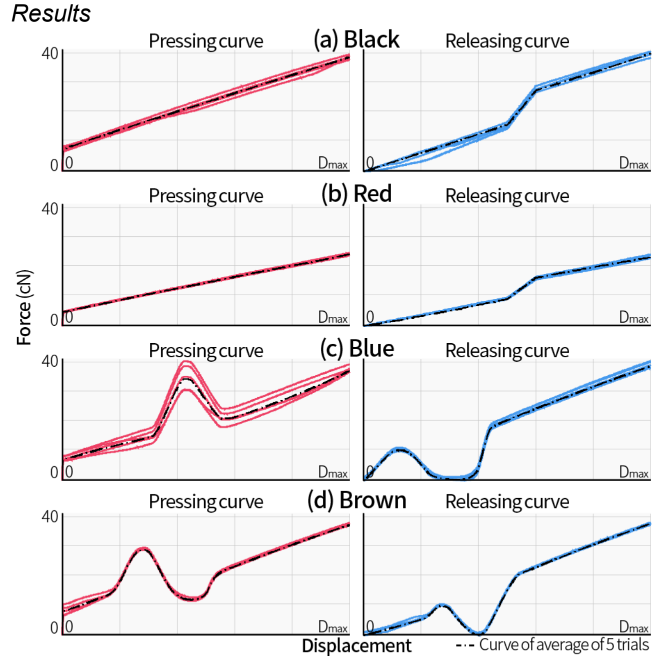


**Figure 8. Normal force measurement results.**

Figure 8 shows the measurement results. The maximum force of **Red** is approximately 25 cN, and that of the rest is approximately 40 cN. The **Blue** pressing curve exhibited the steepest slope of all the curves; however, the measured values in the vicinity of the tactile position fluctuated. Measurements at the peak vary by up to approximately 10 cN. The measured values were not constant in the vicinity of the steep slope; however, a consistent tendency of force change was observed over the five trials. Excluding the **Blue** pressing curve, HapCube provided a generally consistent feedback; thus, the normal feedback of HapCube could reproduce a variety of force–displacement curves.

## MEASUREMENT TEST 2: TO INSPECT INTERFERENCE BETWEEN TANGENTIAL AND NORMAL FEEDBACKS

The measurement tests were conducted to investigate and identify the type of interference that occurs between two feedbacks when they are generated simultaneously.

### Normal Force Measurement

The change in normal force was measured while providing the tangential feedback. The normal feedback was measured while changing the direction of the tangential feedback at 45° intervals. The tangential feedback in each direction was maintained for 10 s. All the other conditions were identical to those in the previous measurement.

#### *Results*

Figure 9 shows the measurement results. Compared to the situation without tangential feedback, the graph in this case is more meandering. However, there is no large difference. Although the tangential feedback was affected by the normal feedback, the normal feedback was not significantly affected by the tangential feedback owing to the difference in the electromagnets' weights. The electromagnet of normal feedback weighs more than twice the electromagnet of tangential feedback.

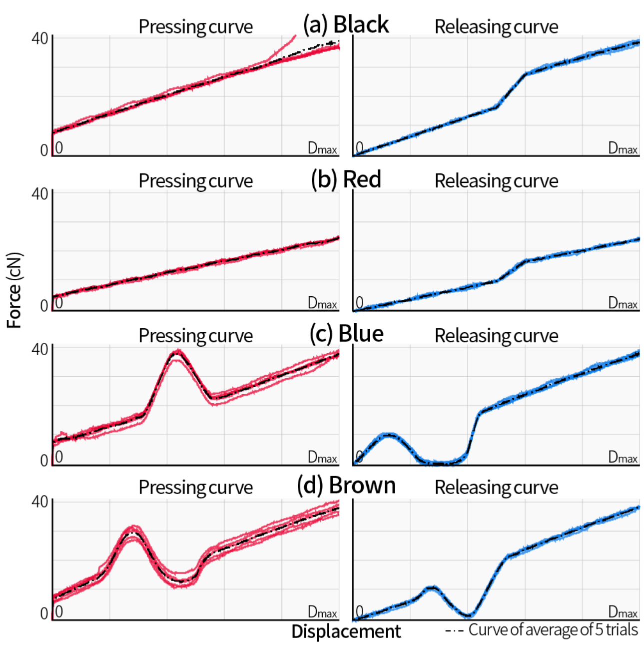


**Figure 9. Normal force measurement with the tangential feedback.**

### Tangential Vibration Measurement

The change in the acceleration of the tangential vibration was measured while providing normal feedback. The normal feedback was generated by increasing and decreasing the voltage from 0 V to 4.5 V and 4.5 V to 0 V for 60 ms each respectively, multiple times. All other conditions were identical to those in the previous measurement.

#### *Results*

Figure 10 shows the measurement results for one of the 16 measured vibrations (the measurement results for all the 16 directions can be downloaded from ACM Digital Library). It was observed that the amplitude of the acceleration and position changed owing to the influence of the normal feedback. As the normal feedback was stronger, the attractive forces between the electromagnet in the normal direction and those in the tangential direction also became stronger lowering the amplitude of vibration. However, the asymmetry of vibration did not vanish.

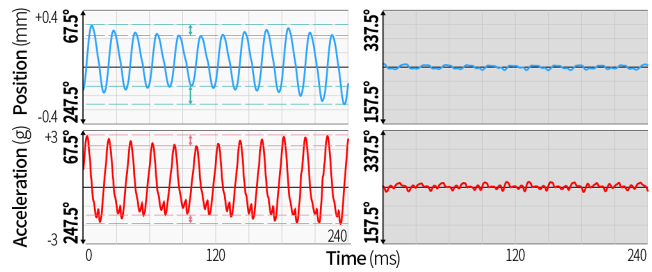


**Figure 10. Tangential vibration measurement with the normal feedback.**

## USER TESTS ON TANGENTIAL FEEDBACK

### Direction Discrimination Test

Participants were asked to identify whether the second virtual force (comparison force) was clockwise or counterclockwise to the first virtual force (standard force) (i.e., 2AFC test) in the presence of two differently directed virtual forces in a sequence. The standard forces were applied in eight directions (at 45° interval), and the comparison forces were applied at ± 20°, ± 45°, and ± 90° to the standard force.

Each pair of standard and comparison forces was presented five times; hence, each participant performed a total of 240 trials (eight standard forces × six comparison forces × five trials). The order of the standard forces was random, and ten (five + and five -) comparison forces were randomly presented for each standard force. The standard and comparison forces were present for 1.5 s each. The participants used the keyboard keys to submit their answers.

The experiment was performed with ten right-handed participants (the mean age: 26.2 y, six females). To minimize learning and fatigue biases, half of the them were assigned to the order of increasing the angle (± 20° to ± 90°) of the comparison force, and the others were assigned to decreasing the angle (± 20° at ± 90°).

#### *Results*

Figure 11 shows the results of the user test. The percentage numbers indicate the correct answers ((a), (b) and (c)). The overall correctness rates for the conditions ± 90°, ± 45°, ± 20° were 97.75%, 95.375%, and 82.25%, respectively. Apparently, a decrease in angle of the comparison force lowers the correctness rate.

In order to estimate the just-noticeable differences (JNDs) in the eight directions, we fitted psychometric functions to proportions of the participant's clockwise answers with a sigmoid equation ($f(x) = 1/(1+e^{-((x-\alpha)/\beta)})$, where $\alpha$ and $\beta$ are constants), and used the least-squares method. In figure 11 (d), the dots are the proportions of clockwise answers, and the S-shaped curves are the fitted psychometric function curves. Each JND value was determined by the difference between the two angles where the curve's proportion values were 0.84 and 0.5. The figure 11 (e) shows the JND values for the eight directions.

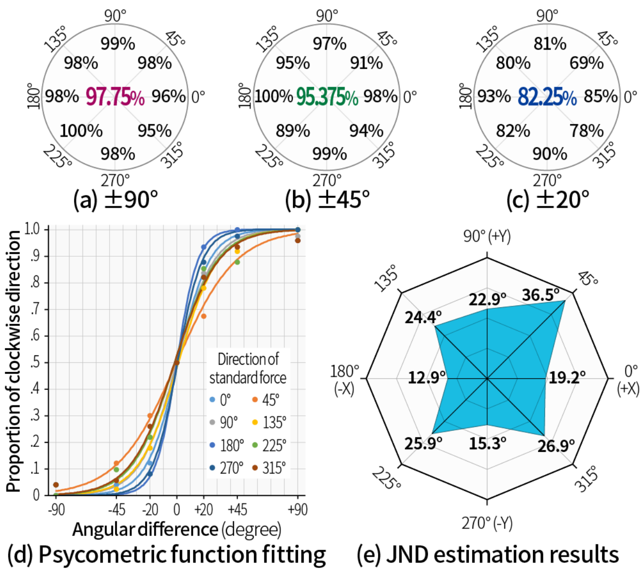


**Figure 11. Direction discrimination test results.**

The range of JND values was 12.9–36.5°, and the results were consistent with the results of previous studies. Amemiya et al. [4] produced a 2D virtual force using a different method and their JND ranges were 11.8–24.7° or 23.1–30.2° depending on the experimental conditions. The JND ranges for real force, not virtual force nor vibration, varied depending on the studies (3.6–11.7° [30], 10.6–15.6° [16], and 23–35° [14]).

Experimental results showed that it was more difficult for the participants to distinguish between the two feedbacks in the diagonal directions. The measurement test results confirm that the diagonal vibration oscillates with a higher amplitude in the orthogonal direction than that in the other directions (Figure 6), which is considered to be the cause for the lower correctness rates and larger JND values in the diagonal directions. Except for the diagonal direction, the results indicated anisotropic cognitive sensitivity. Relatively, it was difficult to accurately recognize the change of angles in the distal direction ($+y$). It was consistent with the results of other previous studies; human finger pads are more sensitive to stretching for the proximal direction [20].

### Direction Detection Test

When the virtual force is applied at random, one participant was asked to identify the correct direction. The test was conducted in three sessions (*four directions*, *eight directions*, and *twelve directions*). In each session, four, eight, and twelve virtual forces were evenly distributed between 0 and 360°. The participant received a virtual force for 1.5 s in a randomly selected direction, and was asked to identify its direction. Each direction was presented five times in random order, thus, a total of 20, 40, and 60 trials were assigned in the three sessions.

The experiment was conducted with ten right-handed participants who did not participate in the discrimination test (the mean age: 25.1 y, four females). To minimize the learning and fatigue biases, half of the participants were tested in the ascending order (*four directions* to *twelve directions*), and the remaining were tested in reverse order.

#### *Results*

Figure 12 shows the results of the direction detection test. The colored area shows the distribution of the participants' answers for each direction. The percentage marked at the center of the circle represents the correctness rate for each session, and the percentage for each direction is the correctness rate for that orientation. The percentages in parentheses are the correctness rates when errors of ± one interval are regarded as correct answers.

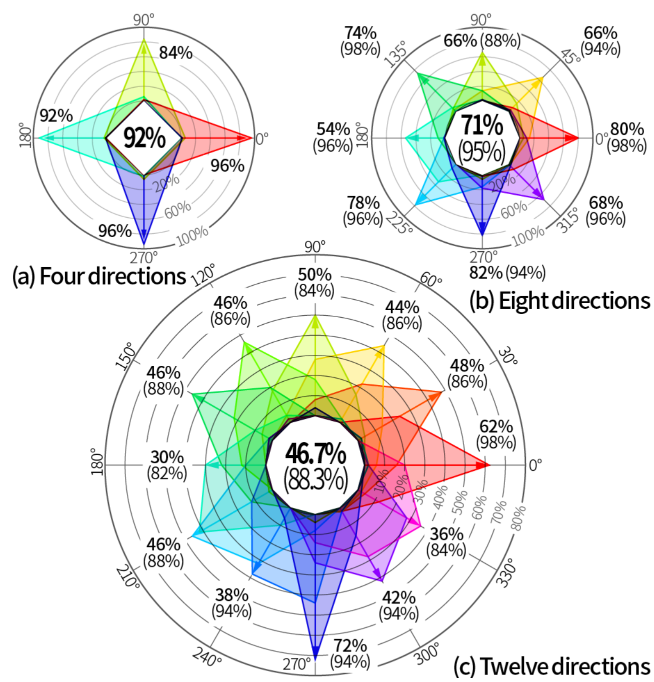


**Figure 12. Direction detection test results.**

The participants were able to distinguish the four directions correctly; they could not do so satisfactorily in case of *eight*, and *twelve directions*. However, the distributions indicate that they did not completely misunderstand the directions. The correctness rates increase significantly when the one-interval errors are allowed, and it means that the participants could perceive the directions, but exhibited difficulty in matching the "perceived direction" to the "precise direction in the real world".

The answers in the 180° direction were widely distributed, and the correctness rate was only 30 %. In Figure 6, it can be seen that the acceleration in the direction of 180° decreases rapidly from the peak in comparison with that in the other directions. The feedback in this direction appears to have a relatively low asymmetry.

## USER TESTS ON NORMAL FEEDBACK

To verify the normal feedback, two user tests were performed to determine if the participants could effectively identify the four virtually simulated key switches (**Black**, **Red**, **Blue**, and **Brown**, shown in Figure 7).

### ABX Test

By pairing the four feedbacks generated by HapCube, six pairs were created (**Black–Red**, **Red–Blue**, **Blue–Brown**, **Brown–Black**, **Black–Blue**, and **Red–Brown**). For example, in a **Black–Red** pair, each participant was provided adequate time to examine the **Black** and **Red** feedbacks prior to ABX testing. Then, one of the **Black** and **Red** was randomly presented and the participant was asked to identify that. The answers were submitted by the participant with the help of the keyboard (by typing one of the 'A' and 'B' keys). Each pair consisted of 12 trials, thus **Black** and **Red** were presented six times each in the **Black–Red** pair. The order of the presented pairs was random.

In this experiment, the bottom-out position ($D_{max}$) was set to 40 mm, and the grain length ($l_g$) was set to 5 mm. The visual feedback used in the experiment was generated with Unity 2017 and The Leap Motion controller. The Leap Motion controller tracked the position of the tip of the index finger wearing the HapCube in real time. Unity displayed a cube-shaped virtual key. It turned green if the fingertip was not touching the cube, tinged-red before the bottom-out position, and blue when it passed the bottom-out position. An identical visual feedback was provided for all the feedbacks.

The update frequency of the system was approximately 120 Hz, and it was challenging to generate feedback by reflecting the position in real time. Therefore, when the fingertip touched the virtual key, the feedback was made to play automatically along the pressing curve for 200 ms, and for 200 ms along the releasing curve when exiting the bottom-out position.

Twelve participants were recruited, of which three were female, and the mean age was 26.5 y (SD: 4.15).

#### *Results*

Table 1 shows the results of the ABX test. The percentages indicate the error rates and the numbers in parentheses indicate the number of participants who did not distinguish between the two feedbacks at 95 % confidence level. In the **Blue–Brown** pair, two participants failed the ABX test, and the error rate was 15.28%. The force–displacement curves of **Blue** and **Brown** were differentiated from the other key feedbacks because they had two tactile positions; however, they were similar to each other. Only **Red** was weak among the four virtual key feedbacks which clearly made **Red** distinct from the other keys. The force–displacement curves of **Black** and **Red** resembled each other; however, they are easily distinguishable because of their unequal strengths. Overall, the participants were able to distinguish the four virtual key feedbacks well.

| | **Black** | **Red** | **Blue** | **Brown** |
|---|---|---|---|---|
| **Black** | | 6.25% (0) | 6.94% (1) | 8.33% (0) |
| **Red** | | | 4.17% (0) | 2.08% (0) |
| **Blue** | | | | 15.28% (2) |
| **Brown** | | | | |

**Table 1. ABX test results**

### Matching Test

Participants were randomly presented one of HapCube's four feedbacks (**Black**$_v$, **Red**$_v$, **Blue**$_v$, and **Brown**$_v$) and were asked to select the most similar one among the four types of the actual CHERRY key switches (**Black**$_p$, **Red**$_p$, **Blue**$_p$, and **Brown**$_p$). When a key feedback was presented, the participants were asked to search for a matching keyboard by pressing the four keyboards (**Black**$_p$: HANSUNG GO187 LED, **Red**$_p$: OZONE OZSTRIKEBATTLE, **Blue**$_p$: LEOPOLD FC200RT, and **Brown**$_p$: FILCO FILCFF02). Ten matching trials were conducted for each feedback, and a total of 40 trials were presented in random order. The setting of the feedback was identical to the ABX test.

The experiment was conducted with ten participants who did not participate in the ABX test, of which three were females, and the mean age was 26.7 y.

#### *Results*

| | | **Black**$_v$ | **Red**$_v$ | **Blue**$_v$ | **Brown**$_v$ |
|---|---|---|---|---|---|
| Answer | **Black**$_p$ | | 8% | 14% | 12% |
| | **Red**$_p$ | 30% | | 0% | 1% |
| | **Blue**$_p$ | 4% | 1% | | 30% |
| | **Brown**$_p$ | 7% | 3% | 38% | |
| | Total | 41% | 12% | 52% | 43% |

**Table 2. Error rate of matching test**

Table 2 shows the error rates of the matching test. When **Black**$_v$ is presented, the answer was **Black**$_p$ in 59 % of the trials (error rate: 41 %). Excluding **Red**$_v$, the percentage of correct answers was approximately 50%. The weak force of **Red**$_v$ was a useful clue for identifying the most similar actual CHERRY switch. Due to this reason, the error rate for **Red**$_v$ was lowest. It was observed that **Blue** and **Brown** were still confusing in comparison with the results of the ABX test. However, the result of **Black**$_v$ with **Red**$_p$ differed from that of the ABX test. In the ABX test, the participants were already aware of the difference in intensity between **Black** and **Red**; however, in this test, the participants did not know the difference between **Red**$_p$ and **Black**$_v$ in advance. Moreover, the maximum repulsive force of **Black**$_v$ was about 40 cN, which was even weaker than the force of **Red**$_p$ (60 cN according to the datasheet). Overall, the matching test was not successful.

## DISCUSSION

### Synthesis of Asymmetric Vibrations

The use of asymmetric vibration has been actively researched because of its capability to provide illusory force sensation without the need to be fastened to the ground. The method of extending the direction of the 1D virtual force multidimension will be a base for various useful applications. Applying the *X-Y* stage structure, we proposed and verified the method to synthesize two orthogonal asymmetric vibrations in a 2D virtual force.

The virtual force in the diagonal direction (including the 180° direction) was confusing when compared to that in the axial direction; we speculate the unidentical damping constant of the four silicone tubes to be the main reason. The results of the tangential vibration measurements showed different patterns of the acceleration and position graphs (Figure 6). It seems to be due to the difference in the dampers rather than in the difference in the magnetic forces of the two electromagnets. The silicone tubes were stretched when they passed through the Case A holes and the plate. The more stretched tubes had higher damping constants and the less stretched tubes had lower damping constants. If the dampers on every axis are designed to be identical (like the rubber membranes of Haptuator [39]), more clear virtual forces can be created in the diagonal directions.

### Reproduction of Compliance

Since human mechanoreceptors are much less sensitive to the skin deformation in the normal direction [17], we could not utilize asymmetric vibration as normal feedback. When the asymmetric vibration was applied in the normal direction, it was perceived as a series of collisions rather than a pulling sensation. Therefore, we applied the Kim et al.'s method [22] to the HapCube. Not to mention the size, the weight also decreased to one-fifth compared to the weight of their prototype. As a voicecoil actuator was used, the actuation delay was almost zero. Through the experiments, we verified that a voicecoil actuator can provide various pseudo-force feedbacks based on the force-displacement curves. However, it failed to distinguish original from the feedback. The matching test results were worse than those of Kim and Lee [23], and Kim et al. [22]. For a more realistic feedback, the shape of the pin and the magnitude of the force should be considered together with the feedback generation method.

### Applications of HapCube

#### *HapCube and Virtual Touch Screen*

Through the interference test, it was found that the normal feedback interferes with the tangential feedback. In order to minimize the interference, the two feedbacks should not be used at same time. In this regard, touch interaction with the virtual touch screens [24,37] can be a good application of HapCube. The normal feedback can be provided when clicking a virtual button and the tangential feedback can be provided when using dragging-or-slide-gestures. Thus, if the provision of two feedbacks is tailored depending on user's touch input, these two feedbacks can work well together in the virtual touch screen situation.

#### *Haptic Navigation Cue of HapCube*

The range of JNDs is 12.9-36.5°, and it is highly consistent with the discrimination thresholds of real force direction of results of previous studies [14,16,30]. Although the correctness rate for twelve directions is about half, the approximate direction of the virtual force was well conveyed. In addition, Figure 11 (b) shows that the participants can easily identify the 45° changes with 95% correctness as shown in Figure 11 (b). Therefore, giving the user a sudden navigation cue in a particular direction (e.g., 22.5° to the right) will confuse the user. However, expectation from navigation is that it tells us when to go right or left. These all results suggest that HapCube can provide enough navigation cue for course modification.

#### *Other Physical Input Devices and HapCube*

The main difference between HapCube and other wearable haptic devices is that the HapCube can function as a haptic actuator. If a large-sized HapCube is developed, it can be used as a hand-held haptic device. In addition, it can be easily embedded into other physical input devices such as VR controller, gamepad, and stylus pen. It can be inserted into any type of device if it can transmit vibrations well.

### Future Work

First, it is necessary to find a method to change the intensity of the virtual force. If we know how to adjust both the direction and the intensity of virtual force, we will be able to provide a more sophisticated feedback to the users.

In addition, a method to combine the tangential and normal feedbacks at a point is necessary. In this study, the tangential and normal feedbacks were transmitted through the plate and the pin; they stimulate different areas of the finger pad. If complete 3-DoF pseudo-force feedback is generated by using vibrations, users will receive more rich and accurate haptic information.

R1 kindly suggested a method to simulate friction and texture simultaneously with the configuration of HapCube. Many methods of changing the roughness of a surface by using vibration that stimulates Pacinian corpuscle have been introduced [5,6,11,28,34]. Since the tangential feedback is stimulating Meissner's corpuscle to render friction, the normal voicecoil actuator can stimulate Pacinian corpuscle to add texture feeling. This method looks feasible and worth trying.

## CONCLUSION

In this study, we showed that two asymmetric vibrations can be synthesized to generate two dimensional virtual forces in a plane. We also demonstrated that it is possible to provide distinctive normal feedback based on compliance curves with a small-sized voicecoil actuator. We hope that the knowledge will be a cornerstone for designing useful haptic device with vibration and human sensory illusion.

## REFERENCES


1. T. Amemiya, H. Ando, and T. Maeda. 2005. Virtual Force Display: Direction Guidance Using Asymmetric Acceleration via Periodic Translational Motion. In *First Joint Eurohaptics Conference and Symposium on Haptic Interfaces for Virtual Environment and Teleoperator Systems*, 619–622. https://doi.org/10.1109/WHC.2005.146
2. T. Amemiya and H. Gomi. 2014. Distinct pseudo-attraction force sensation by a thumb-sized vibrator that oscillates asymmetrically. In *Haptics: Neuroscience, Devices, Modeling, and Applications*. Springer Berlin Heidelberg, 88–95. https://doi.org/10.1007/978-3-662-44196-1
3. Tomohiro Amemiya and Hiroaki Gomi. 2013. Directional Torque Perception with Brief, Asymmetric Net Rotation of a Flywheel. *IEEE Transactions on Haptics* 6, 3: 370–375. https://doi.org/10.1109/TOH.2012.38
4. Tomohiro Amemiya and Hiroaki Gomi. 2016. Active Manual Movement Improves Directional Perception of Illusory Force. *IEEE Transactions on Haptics* 9, 4: 465–473. https://doi.org/10.1109/TOH.2016.2587624
5. Shuhei Asano, Shogo Okamoto, Yoichiro Matsuura, Hikaru Nagano, and Yoji Yamada. 2012. Vibrotactile display approach that modifies roughness sensations of real textures. In *2012 IEEE RO-MAN: The 21st IEEE International Symposium on Robot and Human Interactive Communication*, 1001–1006. https://doi.org/10.1109/ROMAN.2012.6343880
6. Shuhei Asano, Shogo Okamoto, and Yoji Yamada. 2015. Vibrotactile Stimulation to Increase and Decrease Texture Roughness. *IEEE Transactions on Human-Machine Systems* 45, 3: 393–398. https://doi.org/10.1109/THMS.2014.2376519
7. Conrad Bullion and Hakan Gurocak. 2010. Haptic Glove with MR Brakes for Distributed Finger Force. *Presence* 18, 6: 421–433.
8. CHERRY. 2017. *Operation characteristics of CHERRY keyboards*. Retrieved September 16, 2017 from http://www.cherry.de/PDF/EN_CHERRY_MX_Board_5_0.pdf
9. Francesco Chinello, Monica Malvezzi, Claudio Pacchierotti, and Domenico Prattichizzo. 2015. Design and development of a 3RRS wearable fingertip cutaneous device. In *2015 IEEE International Conference on Advanced Intelligent Mechatronics (AIM)*, 293–298. https://doi.org/10.1109/AIM.2015.7222547
10. Jean-Philippe Choiniere and Clement Gosselin. 2017. Development and Experimental Validation of a Haptic Compass Based on Asymmetric Torque Stimuli. *IEEE Transactions on Haptics* 10, 1: 29–39. https://doi.org/10.1109/TOH.2016.2580144
11. H. Culbertson, J. Unwin, B. E. Goodman, and K. J. Kuchenbecker. 2013. Generating haptic texture models from unconstrained tool-surface interactions. In *2013 World Haptics Conference (WHC)*, 295–300. https://doi.org/10.1109/WHC.2013.6548424
12. Heather Culbertson, Julie M. Walker, and Allison M. Okamura. 2016. Modeling and design of asymmetric vibrations to induce ungrounded pulling sensation through asymmetric skin displacement. In *2016 IEEE Haptics Symposium (HAPTICS)*, 27–33. https://doi.org/10.1109/HAPTICS.2016.7463151
13. Heather Culbertson, Julie M. Walker, Michael Raitor, and Allison M. Okamura. 2017. WAVES: A Wearable Asymmetric Vibration Excitation System for Presenting Three-Dimensional Translation and Rotation Cues. In *Proceedings of the 2017 CHI Conference on Human Factors in Computing Systems - CHI '17*, 4972–4982. https://doi.org/10.1145/3025453.3025741
14. Knut Drewing, Michael Fritschi, Regine Zopf, Marc O. Ernst, and Martin Buss. 2005. First evaluation of a novel tactile display exerting shear force via lateral displacement. *ACM Transactions on Applied Perception* 2, 2: 118–131. https://doi.org/10.1145/1060581.1060586
15. Paulo Gallotti, Alberto Raposo, and Luciano Soares. 2011. V-glove: A 3D virtual touch interface. In *Proceedings - 2011 13th Symposium on Virtual Reality, SVR 2011*, 242–251. https://doi.org/10.1109/SVR.2011.21
16. Brian T. Gleeson, Scott K. Horschel, and William R. Provancher. 2010. Perception of Direction for Applied Tangential Skin Displacement: Effects of Speed, Displacement, and Repetition. *IEEE Transactions on Haptics* 3, 3: 177–188. https://doi.org/10.1109/TOH.2010.20
17. Martin Grunwald. 2008. *Human haptic perception : basics and applications*. Birkhäuser. Retrieved January 5, 2018 from https://books.google.co.kr/books?hl=ko&lr=&id=Qmq4BAAAQBAJ&oi=fnd&pg=PP7&dq=human+haptic+perception+basics+and+applications&ots=sLQ2kMU8fp&sig=U7B_n8QvTAuvmTQ70pf4M9ryyik#v=onepage&q=human haptic perception basics and applications&f=false
18. Samantha Horvath, John Galeotti, Bing Wu, Roberta Klatzky, Mel Siegel, and George Stetten. 2014. FingerSight: Fingertip Haptic Sensing of the Visual Environment. *IEEE Journal of Translational*

*Engineering in Health and Medicine* 2372, February: 1–1. https://doi.org/10.1109/JTEHM.2014.2309343

19. Akihiro Imaizumi, Shogo Okamoto, and Yoji Yamada. 2014. Friction Sensation Produced by Laterally Asymmetric Vibrotactile Stimulus. . 11–18. https://doi.org/10.1007/978-3-662-44196-1_2
20. David V. Keyson and Adrianus J. M. Houtsma. 1995. Directional sensitivity to a tactile point stimulus moving across the fingerpad. *Perception & Psychophysics* 57, 5: 738–744. https://doi.org/10.3758/BF03213278
21. Johan Kildal. 2010. 3D-press: Haptic Illusion of Compliance when Pressing on a Rigid Surface. In *International Conference on Multimodal Interfaces and the Workshop on Machine Learning for Multimodal Interaction on - ICMI-MLMI '10*, 8. https://doi.org/10.1145/1891903.1891931
22. Hwan Kim, Minhwan Kim, and Woohun Lee. 2016. HapThimble: A Wearable Haptic Device towards Usable Virtual Touch Screen. In *Proceedings of the 2016 CHI Conference on Human Factors in Computing Systems - CHI '16*, 3694–3705. https://doi.org/10.1145/2858036.2858196
23. Sunjun Kim and Geehyuk Lee. 2013. Haptic Feedback Design for a Virtual Button Along Force-Displacement Curves. In *Proceedings of UIST 2013*, 91–96. https://doi.org/10.1145/2501988.2502041
24. Eunjin Koh, Jongho Won, and Changseok Bae. 2008. Vision-based virtual touch screen interface. *Digest of Technical Papers - IEEE International Conference on Consumer Electronics*: 4–5. https://doi.org/10.1109/ICCE.2008.4587900
25. Thomas H Massie and J K Salisbury. 1994. The PHANTOM Haptic Interface : A Device for Probing Virtual Objects Threee Enabling Observations component of our ability to " visualize ," remember and establish cognitive models of the physical structure of our environment stems from haptic interactions. 1–6.
26. Alvaro G. Perez, Daniel Lobo, Francesco Chinello, Gabriel Cirio, Monica Malvezzi, Jose San Martin, Domenico Prattichizzo, and Miguel A. Otaduy. 2017. Optimization-Based Wearable Tactile Rendering. *IEEE Transactions on Haptics* 10, 2: 254–264. https://doi.org/10.1109/TOH.2016.2619708
27. Jun Rekimoto and Jun. 2013. Traxion: a tactile interaction device with virtual force sensation. In *Proceedings of the 26th annual ACM symposium on User interface software and technology - UIST '13*, 427–432. https://doi.org/10.1145/2501988.2502044
28. Joseph M. Romano and Katherine J. Kuchenbecker. 2012. Creating Realistic Virtual Textures from Contact Acceleration Data. *IEEE Transactions on Haptics* 5, 2: 109–119. https://doi.org/10.1109/TOH.2011.38
29. Rei Sakuragi, Vibol Yem, and Hiroyuki Kajimoto. 2017. Pseudo force presentation to multiple fingers by asymmetric rotational vibration using a motor: Consideration in grasping posture. In *2017 IEEE World Haptics Conference (WHC)*, 305–309. https://doi.org/10.1109/WHC.2017.7989919
30. M. Salada, P. Vishton, J.E. Colgate, and E. Frankel. 2004. Two experiments on the perception of slip at the fingertip. In *12th International Symposium on Haptic Interfaces for Virtual Environment and Teleoperator Systems, 2004. HAPTICS '04. Proceedings.*, 146–153. https://doi.org/10.1109/HAPTIC.2004.1287190
31. Samuel B. Schorr and Allison M. Okamura. 2017. Fingertip Tactile Devices for Virtual Object Manipulation and Exploration. In *Proceedings of the 2017 CHI Conference on Human Factors in Computing Systems - CHI '17*, 3115–3119. https://doi.org/10.1145/3025453.3025744
32. Samuel Benjamin Schorr and Allison M. Okamura. 2017. Three-Dimensional Skin Deformation as Force Substitution: Wearable Device Design and Performance During Haptic Exploration of Virtual Environments. *IEEE Transactions on Haptics* 10, 3: 418–430. https://doi.org/10.1109/TOH.2017.2672969
33. Paul Strohmeier, Jesse Burstyn, Juan Pablo Carrascal, Vincent Levesque, and Roel Vertegaal. 2016. ReFlex: A Flexible Smartphone with Active Haptic Feedback for Bend Input. In *Proceedings of the TEI '16: Tenth International Conference on Tangible, Embedded, and Embodied Interaction - TEI '16*, 185–192. https://doi.org/10.1145/2839462.2839494
34. Paul Strohmeier and Kasper Hornbæk. 2017. Generating Haptic Textures with a Vibrotactile Actuator. In *Proceedings of the 2017 CHI Conference on Human Factors in Computing Systems - CHI '17*, 4994–5005. https://doi.org/10.1145/3025453.3025812
35. Takeshi Tanabe, Hiroaki Yano, and Hiroo Iwata. 2016. Properties of proprioceptive sensation with a vibration speaker-type non-grounded haptic interface. In *2016 IEEE Haptics Symposium (HAPTICS)*, 21–26. https://doi.org/10.1109/HAPTICS.2016.7463150
36. Takeshi Tanabe, Hiroaki Yano, and Hiroo Iwata. 2017. Evaluation of the Perceptual Characteristics of a Force Induced by Asymmetric Vibrations.

*IEEE Transactions on Haptics*: 1–1. https://doi.org/10.1109/TOH.2017.2743717

37. M. Tosas and B. Li. 2004. Virtual Touch Screen for Mixed Reality. In *Computer Vision in Human-Computer Interaction*. 48–59.

38. Jun Wu, Dangxiao Wang, and Yuru Zhang. 2009. Virtual fixture based haptic rendering of handwriting. In *2009 IEEE International Conference on Virtual Environments, Human-Computer Interfaces, and Measurements Systems, VECIMS 2009 - Proceedings*, 16–21. https://doi.org/10.1109/VECIMS.2009.5068858

39. Hsin-Yun Yao and Vincent Hayward. 2010. Design and analysis of a recoil-type vibrotactile transducer. *The Journal of the Acoustical Society of America* 128, 2: 619–627. https://doi.org/10.1121/1.3458852